

Defect Density Dependent Performance Analysis of Perovskite Solar Cell for Different Electron Transport Layers

*Syeda Maria Sultana¹, Mahmudul Hasan², Mosammat Jannatul Ferdous¹,
Israt Jahan Khan Tisha¹, Md. Faysal Nayan^{1*}*

¹Dept. of Electrical and Electronics Engineering, Ahsanullah University of Science and Technology, ²Dept. of Electrical and Electronics Engineering, Northern University Bangladesh

**Corresponding Author*

E-Mail Id: faysal.nayan.eee@aust.edu

ABSTRACT

In recent years, the fourth generation of solar cells, known as hybrid organic-inorganic perovskite solar cells (PSCs), has made significant progress. In PSCs, the absorber layer is made of the economically advantageous material Methylammonium lead halide ($\text{CH}_3\text{NH}_3\text{PbI}_3$). The performance of PSCs depends heavily on the parameters of electron transport material (ETM), absorber layer and hole transport layer (HTL). In this study, Solar Cell Capacitance Simulator (SCAPS)-1D was used to evaluate the performance of perovskite based solar cells for three different ETM Layers: ZnO, TiO_2 and SnO_2 . Furthermore, by varying the defect density of the absorption layer, this study investigated V_{oc} , J_{sc} , FF, and Efficiency. According to the investigation, the J_{sc} , V_{oc} , FF and PCE values of perovskite solar cells decrease drastically when the defect density of the perovskite layer increases. When the defect density went from $1 \times 10^{-15} \text{cm}^{-3}$ to $1 \times 10^{-19} \text{cm}^{-3}$, the power conversion efficiency had significantly reduced from 23% to 3% for TiO_2 , 22% to 6% for ZnO and 22% to 3% for SnO_2 . ZnO as ETM showed the most stability to defect density variation hence discovered to be the most suitable in every scenario for low-cost, high-efficiency solar technology.

Keywords: *Perovskite solar cell, Defect density, Electron Transport Layer, Hole Transport Layer, SCAPS-1D*

INTRODUCTION

The world is heading toward an environmentally friendly solution to its energy challenges as demand rises and fossil fuel supply declines. Most of the energy utilized today is produced by fossil fuels (coal, natural gas, and petroleum products) and this energy supply will run out soon. The hardest job is to create a renewable energy source because fossil fuels have some negative impact on the environment and have finite reserves that are slowly being depleted. The need for renewable energy is expanding as a result of

industrialization and population growth. For this, solar energy is a growing source because it is environmentally friendly and has no negative effects. So, research on energy generating systems using solar cells has gotten a lot of interest and devices using solar energy are needed as a sustainable energy alternative [1][2].

The perovskite solar cell (PSC), a prospective third-generation solar cell (SC), has stimulated research analysis contributing to a significant improvement in power conversion efficiency (PCE). The PSCs' remarkable performance

improvement within a decade has demonstrated their immense potential [3]. The flexibility to gain from the development of related organic and dye-sensitized photovoltaic cells over a 20-year period, as well as simplicity of fabrication, substantial solar absorption, reduced non-radiative carrier recombination rates for materials that are so easily made, have high power conversion efficiencies (PCE), and may have cheap manufacturing costs in bulk quantities are some key characteristics of these Perovskites [4].

Additionally, PSC may be highly light, flexible and thin, which expands the range of uses for this kind of cutting-edge solar devices. Maximizing the efficiency to the cost ratio while developing photovoltaic solar cells is the key problem. A valuable tool for understanding physics of the PV device and analyzing the effects of different variables on performance is numerical simulation. It is clear that the simulation analysis provides an idea to maximize solar cell performance [5].

The heterojunction architecture of the planar PSC typically consists of three primary layers: the Perovskite absorber, the hole transport material, and the electron transport material (ETM) (HTM). TiO_2 , $\text{CH}_3\text{NH}_3\text{PbI}_3$, and Spiro-OMeTAD are the most often utilized ETM, Perovskite, and HTM, respectively [3]. Mesoporous TiO_2 is typically used as the buffer layer in organic-inorganic Perovskite solar cells to boost light absorption. However, TiO_2 , which also has strong electrical properties to use as a buffer layer, can be successfully replaced with ZnO [6]. Even though Perovskite absorber layers have many benefits, flaws still affect how well PSCs function because they cause hysteresis, non-radiative recombination, charge trapping, charge scattering and ion migration [7].

When it comes to solution-processed Perovskite solar cells, the defective states typically start during the material and device processing and are usually inevitable [8].

Depending on where they are located in the energy band gap, defects can be categorized. They may be shallow or deep, and they may also be categorized as donors or acceptors. Deep-level errors are particularly to blame for the cell's bad performance among these flaws [9]. The characteristics of defects, particularly point (Schottky and Frenkel) flaws, in absorbers are crucial in determining the V_{oc} (open circuit voltage) and an electron-hole diffusion length of a solar cell. Deep level defects typically function as Shockley-Read-Hall nonradiative recombination centers, which contributes to the minority carrier lifetime being short and the resulting poor V_{oc} [10]. The defect densities of Perovskite are precursor, partial-pressure, temperature and formation energy-dependent, resulting in chemical potential. Low formation energy defects only produce shallow levels, resulting in high V_{oc} and extended electron-hole diffusion lengths. Conversely, deep level faults have a large formation energy, which has an inverse impact on V_{oc} and the length of the electron-hole diffusion [11].

Deep defect levels in the Perovskite are depicted in a number of publications at energies of 0.24 and 0.65 eV below the conduction band (CB) and 0.17, 0.28, and 0.5 eV above the valence band (VB). One of the causes of the hysteresis issue in PSC is Frenkel flaws, which are most frequently found in Perovskites. Potential-induced degradation, which has a negative impact on the performance of a number of thin-film solar cells, including copper zinc tin sulfide (CZTS), copper indium gallium selenide (CIGS), and copper zinc tin sulphur-selenium

alloy, can also accumulate defects (CZTSSe) [9].

DEVICE STRUCTURE

To do the simulations, SCAPS (Solar Cell Capacitance Simulator), a 1D solar cell simulation tool, is employed [12]. The typical PSC p-i-n formation is depicted in Figure 1 where it depicts the solar cell's schematic architecture and is constructed with five layers. In this work, the

CH₃NH₃PbI₃ (MAPbI₃) is used as a Perovskite layer which sits between both the layers of HTM and ETM. The cells front and back contacts are Fluorine doped Tin Oxide (FTO) and Ag/Al, respectively. NiO_x is used in every structure for HTM, as was already mentioned. Three different metal oxides, TiO₂, ZnO, and SnO₂, that are alternatively used as the ETM layer

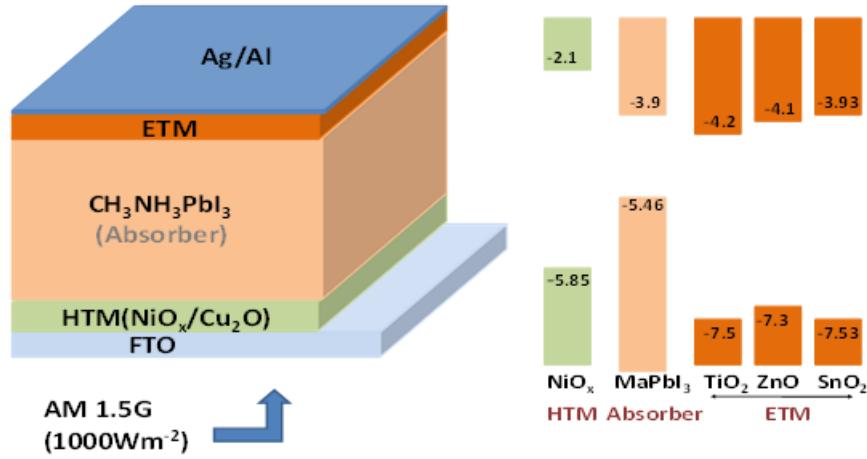


Fig. 1: PSC Structure schematic design for the simulation. The top and the lower halves of the right-hand figure, which stand for CB and VB, respectively, show the materials' band alignment.

The recombination rate (R) can be represented as follows in the SRH model:

$$R_{SRH} = \frac{n_p - n_i^2}{\tau_n(n + n_i) + \tau_p(p + n_p)} \quad (1)$$

Where τ_n is the electrons lifetime and τ_p is holes lifetime, n_i is the intrinsic density.

The ratio of the maximum power output ($P_{out} = J_{MPP}V_{MPP}$) to the power input is known as the solar cell's (P_{in}) power conversion efficiency (PCE) [13]. PCE can be expressed as

$$PCE = \frac{FFJ_{sc}V_{oc}}{P_{in}} \quad (2)$$

The open-circuit voltage is calculated using [14]:

$$V_{oc} = \frac{kT}{q} \ln \left(\frac{J_{sc}}{J_0} + 1 \right) \quad (3)$$

SIMULATION SETUP

The simulation's parameters were chosen after reading relevant literature. Table-1 lists all of the simulation's input parameters, while Table 2 contains statistics on defects level which used in

simulation. Solar cells based on $\text{CH}_3\text{NH}_3\text{PbI}_3$ (MAPbI₃) are simulated at AM1.5G at 300K. The parameter values of different layers are meticulously derived through studies [14].

Table 1: Parameters of different layers in SCAPS [14]

Properties	NiOx	Perovskite	ZnO	SnO ₂	TiO ₂
Thickness (nm)	80	455	70	60	60
Bandgap (eV)	3.7	1.56	3.2	3.6	3.2
Affinity (eV)	2.1	3.9	4.1	4.07	4.2
Dielectric Permittivity	10.7	10	10	8	10
DOS of CB ($1/\text{cm}^3$)	2.8×10^{19}	2×10^{18}	4.5×10^{18}	3.16×10^{18}	2.5×10^{18}
DOS of VB ($1/\text{cm}^3$)	1.8×10^{19}	1×10^{18}	1×10^{18}	2.5×10^{19}	1×10^{18}
Electron mobility (cm^2/vs)	12	100	150	75	0.7
Hole mobility (cm^2/vs)	25	10	1	0.1	0.1
Acceptor Concentration ($1/\text{cm}^3$)	2×10^{14}	1×10^9	0	0	0
Donor Concentration ($1/\text{cm}^3$)	0	1×10^9	1×10^{16}	1×10^{18}	9×10^{17}

Table 2: Parameters of defects level [14]

The defect levels used in our simulation		
Defect type	MAPbI ₃ layer bulk defect	ETM Layer bulk defect
Electron capture cross section (cm^2)	1×10^{-15}	1×10^{-15}
Hole capture cross section (cm^2)	1×10^{-15}	1×10^{-15}
Energetic distribution	Gauß	Gauß
Energy level with respect to Ref (eV)	0.75	0.5
Total defect density (cm^{-3})	1×10^{-17}	1×10^{-15}

SIMULATION RESULT

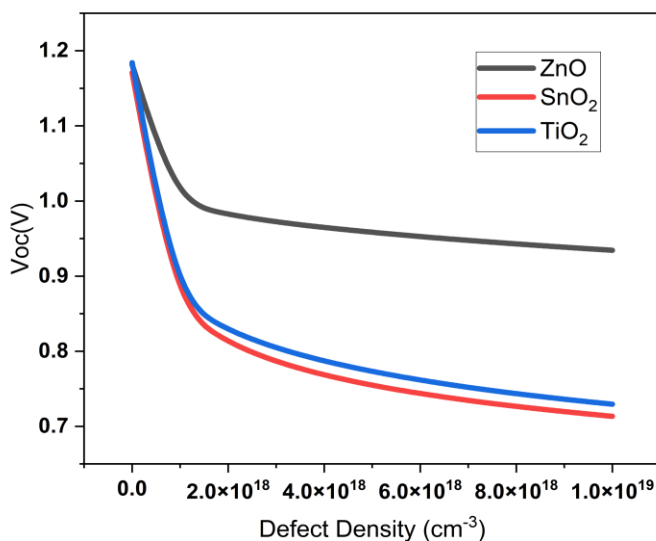


Fig. 2: Varying Voc with the total defect density

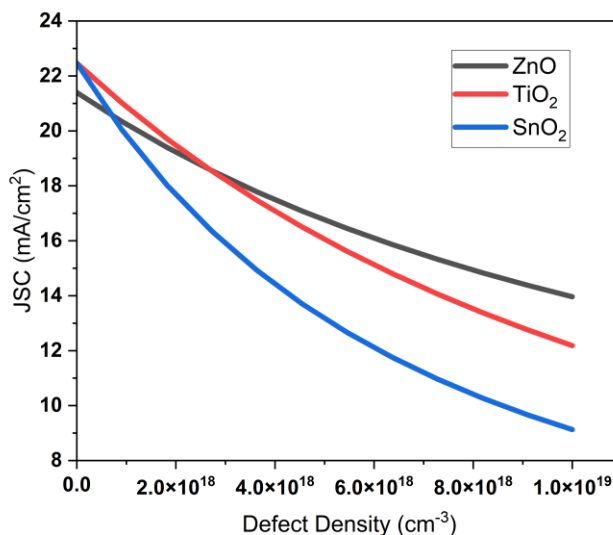


Fig. 3: Varying Jsc with the total defect density

We are emphasizing on one of the most performance limiting elements for a solar cell in this section: defects in the absorber layer. Imperfections and limitations in the fabrication process lead to defects. Between the valence and conduction bands, the absorber layer's defects form transitional energy levels which function as "trap centers" that eventually lead to Shockley-Read-Hall (SRH) recombination, the recombination of

carriers. This reduces carrier lifetime, which leads to lower photocurrent and less effective cells [13].

To observe this effect, the performance is assessed as shown in Fig. 2 to Fig.5, with the defect density of the Perovskite layer (bulk defect) ranging from $1 \times 10^{18} \text{ cm}^{-3}$ to $1 \times 10^{19} \text{ cm}^{-3}$. As expected, all properties exhibit deteriorating performance as the defect level rises.

Figure.2 shows a drop in V_{oc} as the defect density increases. For SnO_2 and TiO_2 , V_{oc} changes from 1.18V to 0.7V but for ZnO to 0.93V. There is also decrement in the J_{sc} as shown in Fig.3 with increasing absorber layer defect density. J_{sc} for ZnO,

SnO_2 and TiO_2 decreases from 21.4 to 14 mAcm^{-2} , 22.5 to 9.1 mAcm^{-2} and 22.5 to 12.2 mAcm^{-2} respectively.

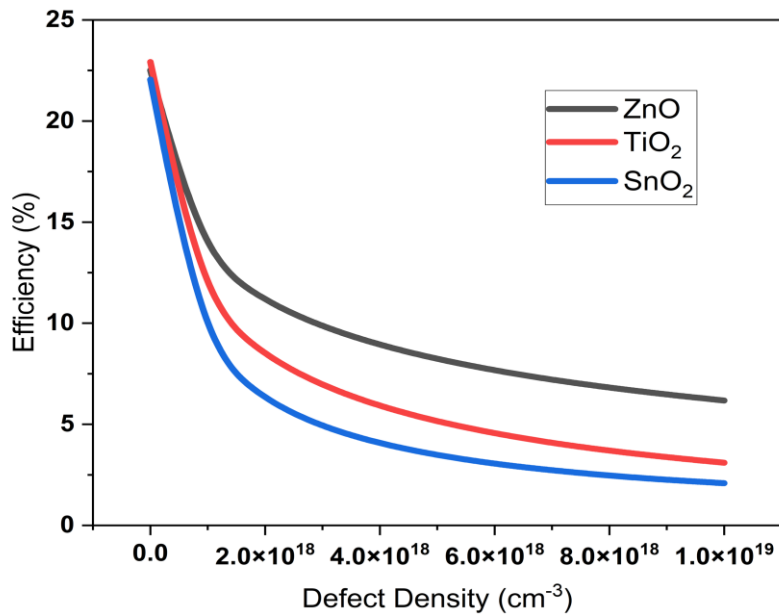


Fig. 4: Varying efficiency with the total defect density

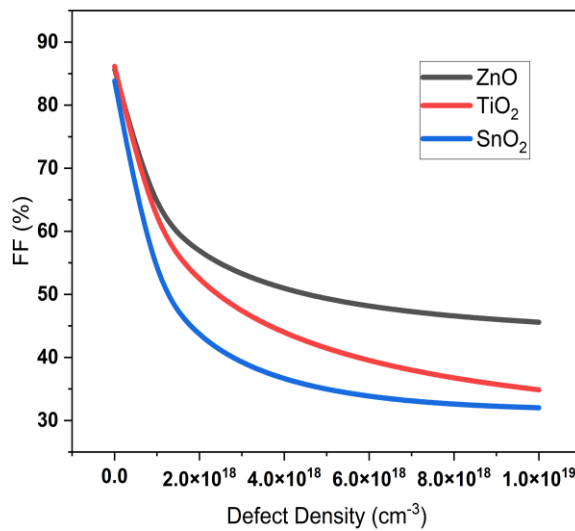


Fig. 5: Varying FF with the total defect density

Increasing the defect density results in decreasing the devices efficiency represented as PCE which is shown in Fig.4. TiO₂ has the highest efficiency of 23% at the beginning but soon decreases to 3%. ZnO and SnO₂ shows the same pattern by decreasing from 22% to 6% and 3% respectively. The decreasing pattern is also true for FF which can be seen in Fig.5. For the three

ETMs ZnO, SnO₂ and TiO₂ the highest and lowest values of FF are 85% to 45%, 83% to 32% and 86% to 35% respectively.

The device's Voc is decreased by the drop in shunt resistance that results from the defect induced recombination centers [15]. Since shallow defects impede carrier mobility and lower charge carrier

collection, Jsc is more affected than Voc. A reduction in carrier density for photocurrent results from more photo-generated carriers becoming trapped as defects accumulate. As FF depends highly on Voc and higher voltage will have a higher possible FF with a decrement in Voc, FF also decreases. Low defect density increases diffusion length, which decreases carrier loss through recombination and enhances cells performance.

On the other hand, an increased defect density results in a shorter diffusion length, which accelerates the rate of charge carrier recombination. Thus, the cell's efficiency declines and performance therefore suffers greatly.

Table 3: Performance characteristics of three ETMs' p-i-n perovskite solar cell architectures

Structure	Open Circuit Voltage (V)		Short Circuit Current (mAc_m-2)		Fill Factor (%)		Efficiency (%)	
	Max	Min	Max	Min	Max	Min	Max	Min
with ZnO	1.18	0.93	21.4	14	85	45	23	6
with TiO₂	1.06	0.7	22.5	9.1	83	35	22	3
with SnO₂	1.17	0.7	22.5	12.2	86	32	22	3

Table 3 represents the highest and the lowest value of VOC, JSC, FF and ETA for three ETM layers. ZnO shows the highest VOC and efficiency, TiO₂ shows the highest JSC nad FF and SnO₂ shows the highest JSC.

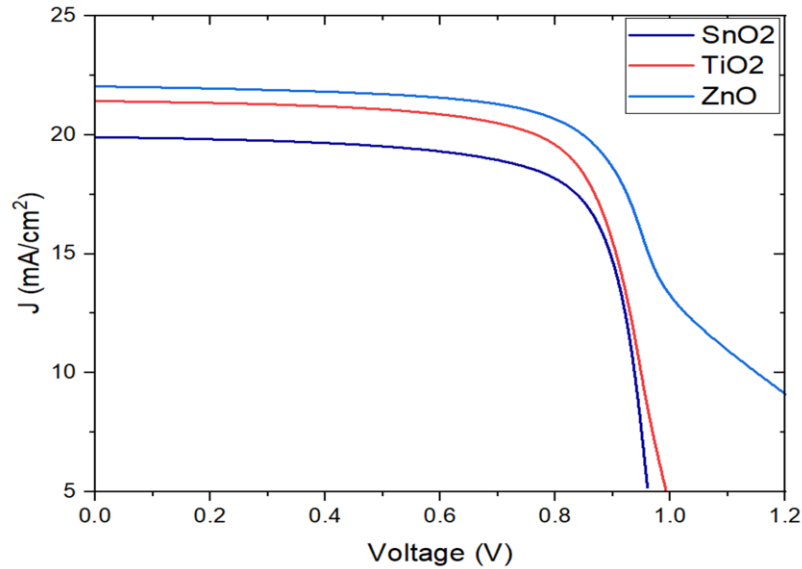


Fig. 6: Three ETM layers' I-V characteristic curve

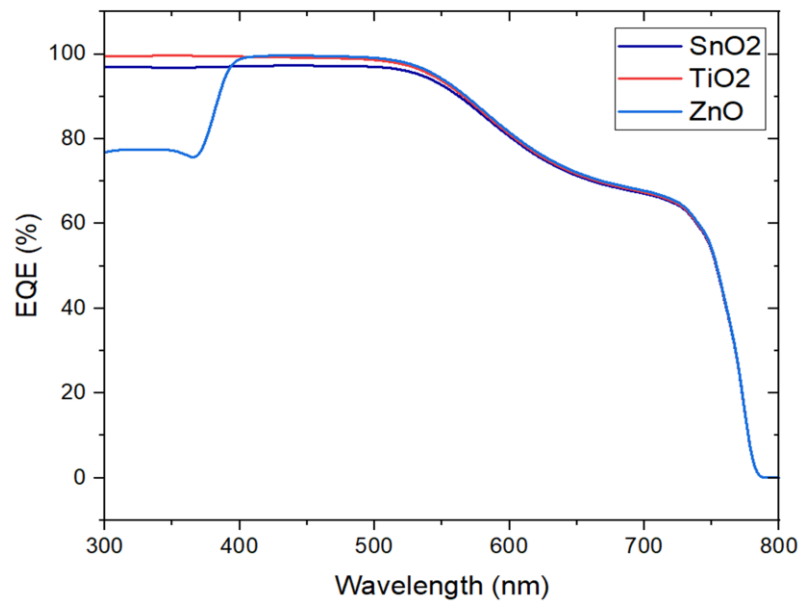


Fig. 7: Varying quantum efficiency with wavelength

Fig.6. displays the current-voltage characteristics for three distinct ETM layers. An essential characteristic of a high-performance solar cell is the ability to absorb photons and successfully convert them into electrons in both the UV and visible spectrum. Fig.7. displays the

optical properties of the perovskite solar cell. The greatest photon-to-electron conversion ratio, or QE, for wavelengths between 380 nm to 690 nm for ZnO. On the other hand, for TiO₂ between 300nm to 700nm and for SnO₂ 300nm to 610 nm wavelength region, the figure depicts the

greatest photon to electron conversion ratio or QE. After the wavelength of 760nm, the quantum efficiency declines dramatically for all of them. The quantum efficiency in this scenario decreases from 80% to 0% for ZnO. On the other hand, for TiO₂ and SnO₂ the quantum efficiency decreases from 99% to 0% [1].

Among the ETMs ZnO shows better stability in terms of defect density variation. In addition to its high transmittance in the visible spectrum and low cost, Zinc oxide also has a substantially greater electron mobility of 115–155 cm²v⁻¹s⁻¹, which has the potential to increase the efficiency of electron transport and decrease recombination loss as an ETM.

CONCLUSION

This paper presents a simulation-based research of a Perovskite (CH₃NH₃PbI₃)-based solar cell with a simple n-i-p structure and three distinct ETM layers: ZnO, SnO₂, and TiO₂. The literature is used to derive consistent material parameters. The HTM for all simulated structures, NiO_x, performs well due to its enhanced optical transparency (larger bandgap) and effective carrier collection. The current work investigates how the defect density of the absorber layer and the use of various electron transport layers affect photovoltaic performance.

From our results, we can conclude that the absorbers defect density has a significant impact on the performance of the solar cell as increasing defect density results in lower Voc, Jsc, FF as well as ETA or efficiency. It is due to the fact that absorber layer defects create trap energy levels which leads to a higher recombination rate of charge carriers and poor cell performance. ZnO exhibits more tolerance to absorber bulk defect variation than the other two ETMs. Even at higher levels efficiency of ZnO based cells are

superior than SnO₂ or TiO₂. The underlying reason behind this can be that ZnO has a greater electron mobility that can decrease the recombination loss by increasing the electron transport efficiency. Conclusively the simulation study suggests that by using ZnO as ETM layer and keeping the defect density as minimum as possible, maximum efficiency and cell performance can be attained.

FUTURE SCOPE

In this paper, the defect density varied in a small range due to observe the effect. Next the defect density will be varied in a large range and observed the effect in VOC, JSC, ETA and FF.

REFERENCES

1. P. K. Patel, "Device simulation of highly efficient eco - friendly - perovskite solar cell," Sci. Rep., pp. 1–11, 2021.
2. B. M. Soucase, I. G. Pradas, and K. R. Adhikari, "Numerical Simulations on Perovskite Photovoltaic Devices," 2016.
3. G. Haidari, "Comparative 1D optoelectrical simulation of the perovskite solar cell Comparative 1D optoelectrical simulation of the perovskite solar cell," vol. 085028, no. August, 2019.
4. M. A. Green, A. Ho-baillie, and H. J. Snaith, "The emergence of perovskite solar cells," vol. 8, no. July, 2014.
5. D. Swisulski, "Simulation investigation of perovskite-based solar cells," no. 5, pp. 99–102, 2021.
6. F. Hossain, M. Faisal, and H. Okada, "Device Modeling and Performance Analysis of Perovskite Solar Cells Based on Similarity with Inorganic Thin Film Solar Cells Structure," no. December, pp. 8–10, 2016.
7. S. Mahjabin, M. Haque, K. Sobayel, M. S. Jamal, M. A. Islam, and V.

- Selvanathan, "Perceiving of Defect Tolerance in Perovskite Absorber Layer for Efficient Perovskite Solar Cell," vol. XX, pp. 1–10, 2020.
8. V. Srivastava, S. H. Reddy, B. Anitha, and A. G. Manoj, "A comparative study of defect density of states for single, mixed and bulk heterojunction perovskite solar cells A Comparative Study of Defect Density of States for Single, Mixed and Bulk Heterojunction Perovskite Solar Cells," vol. 050013, no. March, 2019.
 9. P. S. Cell, "Design, Performance, and Defect Density Analysis of Efficient Eco-Friendly," vol. 67, no. 7, pp. 2837–2843, 2020.
 10. W. Yin, T. Shi, Y. Yan, W. Yin, T. Shi, and Y. Yan, "Unusual defect physics in $\text{CH}_3\text{NH}_3\text{PbI}_3$ perovskite solar cell absorber," vol. 063903, 2014.
 11. A. Manuscript, "Materials Chemistry A," 2014.
 12. "SCAPS: Home." <http://www.scaps.com/> (accessed Oct. 16, 2022).
 13. N. Chawki, "Numerical Study of BaZrS_3 Based Chalcogenide Perovskite Solar Cell Using SCAPS-1D Device Simulation," pp. 1–18, 2022.
 14. M. S. Rahman, S. Miah, M. S. W. Marma, and T. Sabrina, "Simulation based Investigation of Inverted Planar Perovskite Solar Cell with All Metal Oxide Inorganic Transport Layers," 2nd Int. Conf. Electr. Comput. Commun. Eng. ECCE 2019, no. May, 2019.
 15. N. Singh, A. Agarwal, and M. Agarwal, "Numerical simulation of highly efficient lead-free all-perovskite tandem solar cell," Sol. Energy, vol. 208, no. August, pp. 399–410, 2020.